RADIATION STUDIES OF METAL-OXYGEN MIXTURES

M. G. Dunn, et al

Calspan Corporation

Prepared for:

Defense Nuclear Agency
Defense Advanced Research Projects Agency

1 August 1975

DNA 3624F

RADIATION STUDIES OF METAL-OXYGEN MIXTURES

Calspan Corporation
P.O. Box 235
Buffalo, New York 14221

1 August 1975

Final Report for Period 27 February 1974—31 January 1975

CONTRACT No. DNA 001-74-C-0220

APPROVED FOR PUBLIC RELEASE;
DISTRIBUTION UNLIMITED.

THIS WORK SPONSORED BY THE DEFENSE NUCLEAR AGENCY UNDER SUBTASKS S99QAXHI002-19 AND M99QAXHI002-01, IN COOPERATION WITH THE DEFENSE ADVANCED RESEARCH PROJECTS AGENCY UNDER DARPA ORDER NUMBER 1433.

Prepared for

Director
DEFENSE NUCLEAR AGENCY
Washington, D. C. 20305

UNCLASSIFIED

SECURITY CLASSIFICATION OF THIS PAGE (When Data Entered)

REPORT DOCUMENTATION PAGE		READ INSTRUCTIONS BEFORE COMPLETING FORM
1 REPORT NUMBER DNA 3624F	2. GOVT ACCESSION NO.	3 RECIPIENT'S CATALOG NUMBER
4 TITLE (and Subtitle) RADIATION STUDIES OF METAL-OXYGEN MIXTURES		5. TYPE OF REPORT & PERIOD COVERED Final Report for Period 27 Feb 74—31 Jan 75 6 PERFORMING ORG. REPORT NUMBER WB-5487-A-1
7 AUTHOR(s) M. G. Dunn C. E. Treanor W. H. Wurster		8 CONTRACT OR GRANT NUMBER(s) DNA 001-74-C-0220
9 PERFORMING ORGANIZATION NAME AND ADDRESS Calspan Corporation P.O. Box 235 Buffalo, New York 14221		10 PROGRAM ELEMENT, PROJECT, TASK AREA & WORK UNIT NUMBERS NWER Subtask S99QAXHI002-19 NWER Subtask M99QAXHI002-01
11 CONTROLLING OFFICE NAME AND ADDRESS Director Defense Advanced Research Projects Agency (DARPA) Washington, D.C. 20305		12 REPORT DATE 1 August 1975 13 NUMBER OF PAGES 48
14 MONITORING AGENCY NAME & ADDRESS(if different from Controlling Office) Director Defense Nuclear Agency Washington, D.C. 20305		15 SECURITY CLASS. (of this report) UNCLASSIFIED 15a. DECLASSIFICATION/DOWNGRADING SCHEDULE

16 DISTRIBUTION STATEMENT (of this Report)

Approved for public release; distribution unlimited.

17 DISTRIBUTION STATEMENT (of the abstract entered in Block 20, if different from Report)

18 SUPPLEMENTARY NOTES

This work sponsored by the Defense Nuclear Agency under Subtasks S99QAXHI002-19 and M99QAXHI002-01, in cooperation with the Defense Advanced Research Projects Agency under DARPA Order Number 1433.

19 KEY WORDS (Continue on reverse side if necessary and identify by block number)

Metal Oxides	Equilibrium Radiation
Uranium	High Temperature
Infrared	Aluminum
Quantitative Spectra	Fundamental Bands

20 ABSTRACT (Continue on reverse side if necessary and identify by block number)

Many problems involving the prediction of radiance from heated gases or plasmas containing metals and their oxides are limited in the reliability of their solution because relevant spectroscopic properties of the radiating species are not known. Despite significant recent advances in calculational procedures, many cases still require experimentally based data for reliable inputs to radiance predictions. This is especially true in the infrared spectral range.

DD FORM 1 JAN 73 1473 EDITION OF 1 NOV 65 IS OBSOLETE

UNCLASSIFIED

SECURITY CLASSIFICATION OF THIS PAGE (When Data Entered)

10. PROGRAM ELEMENT, PROJECT, TASK AREA & WORK UNIT NUMBERS (Continued).

DARPA Order Number 1433, Amendment 10, Program Code Number 4E50, Program Element Code 62301F.

20. ABSTRACT (Continued).

The research program discussed in this Final Report was an outgrowth and extension of studies conducted through June 1973 for the Defense Advanced Research Projects Agency under Contract No. DNA 001-72-C-0098. The purpose of these studies was to provide quantitative spectrometric measurements for metal oxide species in the IR. They are intended to provide a broad data based upon which radiative models may be built for reliable predictions of radiation for a chemical system containing uranium and/or aluminum and oxygen under a variety of environmental conditions.

Measurements have been made with both aluminum and uranium, using the Calspan aerosol shock tube, which has been equipped with a cooled-optics test section for overall increased detectivity in the infrared around 10 μm. In the aluminum/oxygen mixture, absolute radiance levels were measured simultaneously in the Blue-Green ($B \rightarrow X$) visible bands and the fundamental vibration band near 10 μm. The ratio of these radiances is independent of the AlO molecular concentration, and its variation with temperature can be reliably predicted. Using available values for the transition probabilities of the ($B \rightarrow X$) system yields at 10 μm band strength which is greater than recently published data by a factor of two. Preliminary infrared results with uranium indicate that by comparison, with the AlO, the radiance levels from the uranium/oxygen system are significant and warrant further study.

PREFACE

This is the Final Report on Contract DNA 001-74-C-0220 and covers the period 27 February 1974 through 31 January 1975. This work was sponsored by the Defense Advanced Research Projects Agency and by the Defense Nuclear Agency (FY75).

Contributors to the research reported herein were Drs. C. E. Treanor, W. H. Wurster, and M. G. Dunn of the Aerodynamic Research Department at the Calspan Corporation.

Technical monitoring of this research was done by Dr. Charles A. Blank of the Defense Nuclear Agency.

The authors wish to acknowledge the assistance of Miss Marcia Williams in the calculation of radiation parameters necessary in the data reduction procedure.

TABLE OF CONTENTS

LIST OF ILLUSTRATIONS

SECTION 1

INTRODUCTION

Several methods have been reported which address the problem of obtaining metals and metal oxides in gaseous mixtures for spectroscopic studies. They include ground metal slurrys on substrates, the use of metal-organic compounds, and particulate dust injection[1,2]. For spectroscopic studies, it can be appreciated that the use of any substances other than the pure metal of interest results in overlapping, contaminated spectra which can seriously compromise the subsequent analyses. This is especially true for IR measurements, where the use of photographed spectra is precluded, and the identification and subtraction of radiating species in contaminated spectra is rendered prohibitively difficult.

The method developed at Calspan, which is described briefly in the following section, has been shown to produce very clean spectra. In aluminum, for example, the visible spectrum contains only atomic Al resonance lines and the blue-green band system of AlO . No hydrocarbon species were present, the usual Na and Ca lines were the only background radiators. This technique was initially used[3,4] in order to measure the band strength of U - O_2 mixtures in the LWIR using a Hg:Cd:Te detector. However, the performance of the initial system was limited because of an effective background temperature of about 350°K. As a result of these early studies, it was recommended that a liquid helium cooled Ge:Hg detector and filter used in conjunction with a liquid nitrogen cooled test section would significantly improve the sensitivity of the system in the LWIR. Therefore, a new test section capable of being cooled with liquid nitrogen was designed and constructed, and the recommended cold optics was incorporated. The results reported herein were obtained with this new system.

A discussion of the experimental method and a description of the apparatus is presented in Section 2. The results obtained to date, including a discussion of the data reduction procedure and a comparison of these results with other data, are presented in Section 3.

SECTION 2

EXPERIMENTAL APPARATUS

A schematic diagram of the apparatus used for the radiance measurements is shown in Figure 1. The essential features are the shock tube, the aerosol generator, the liquid-helium cooled mercury-doped germanium infrared detector and the liquid-nitrogen cooled test section at the reflected-shock end of the tube which provides a cold optical train and background for this detector. The band-stremgth measurements are performed on the reflected-shock processed gas. The test gas comprises a noble carrier gas such as argon with varying amounts of oxygen and an aerosol of the pure metal under study. This mixture is shock heated; the aerosol particles evaporate in a time which is short compared with the shock-tube test time, producing a processed test gas consisting only of the atoms and oxide molecules of the metal under study.

The shock tube is a conventional pressure-driven tube. It is constructed of stainless steel with a honed 2-in. inside diameter, and a driven-tube section 11-ft. in length. Flow is initiated in the driven section using the double-diaphragm technique for good reproducibility of test conditions. The wave speed is measured over four intervals (the first interval is 1-ft. and the remaining three intervals are 2-ft.) using electronic counters actuated by signals from heat-transfer gauges. Additional wave-speed measurements were obtained with an ionization gauge located in the shock-tube end wall. The results of the five-interval measurements were in excellent agreement with those obtained with four wave-speed intervals, and permitted an accurate history of the shock-wave velocity to be obtained.

2.1 AEROSOL CHAMBER AND AXIAL DISTRIBUTION OF AEROSOL

The technique used here to introduce the aluminum or uranium particles into the shock tube is the same as that previously described by Wurster[3,4]. The method consists of exploding a segment of the desired material in a controlled atmosphere (aerosol generator), thereby producing a metallic smoke or aerosol. The aerosol generator is located at the test-section end of the shock tube as

shown. This generator is an aluminum cylinder, 4-in. in diameter by 4-in. in length, with a volume equal to approximately 0.10 that of the shock tube, and which contains two electrodes for clamping the wire that is to be exploded. The energy used to explode the wire is about 30 J., using a potential of 7500 V. Initially, the aerosol generator and the shock tube are at a pressure of approximately 5×10^{-5} torr. Shortly after the test gas is introduced into the aerosol chamber, the wire is exploded forming solid particles of $Al_2 O_3$ in the case of aluminum. A motor driven valve then opens which permits the aerosol to expand into the driven-tube section and established the required initial pressure for the test gas. The valve is then closed and after approximately a one or two-minute delay the double-diaphragm unit is vented and the experiment takes place. The $Al_2 O_3$ particles are vaporized by shock heating and the appropriate aluminum-oxygen species are formed. The resultant freedom from condensation problems gives rise to the inherently greater range of chemical systems that can be addressed by the aerosol technique.

The aerosol distribution behind the incident shock is monitored at four locations along the driven-tube section by using a single photomultiplier tube as illustrated in Figure 1. For the experiments reported here, a 5086 to 5142 A filter was placed in the field of view of the photomultiplier so that the AlO radiance from the $\Delta v = 1$ band sequence would be monitored. The received signals from each of these spatial positions were calibrated by using a light source in the tube. This calibration procedure permitted normalization corrections to be made to the results shown in Figure 2.

Figures 2(a) and (b) are typical of the results obtained behind the incident shock in the wavelength region 5086 to 5142 A. Both data records were obtained for an initial shock-tube pressure of 25 torr of 94.9% Argon plus 5.1% oxygen. However, Figure 2(a) was obtained for an experiment in which aluminum had been added to the test gas and Figure 2(b) was obtained in the absence of aluminum. These results illustrate the chemical purity of the system and the fact that the radiation observed in Figure 2(a) is attributable to AlO .

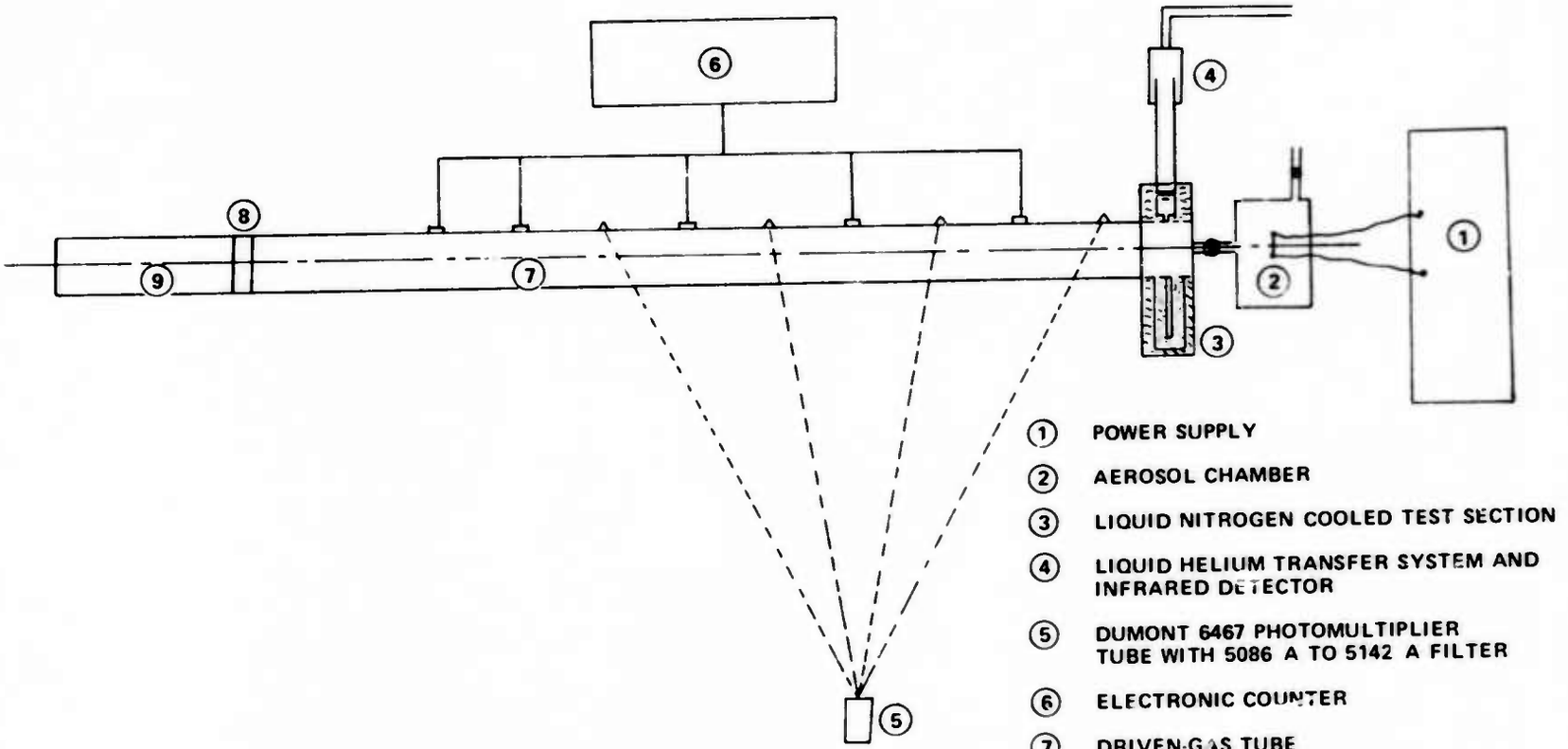

Figure 1. Schematic of experimental apparatus.

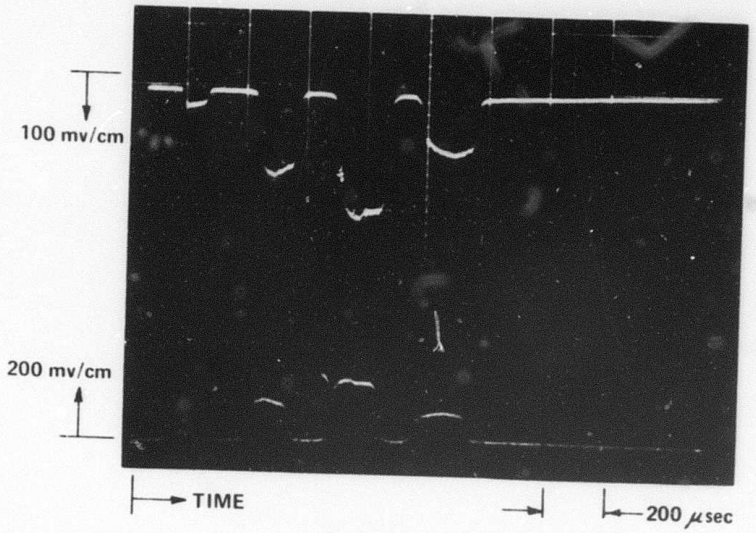

a) WITH A ℓ IN TEST GAS

TEST GAS: 25 torr
94.9% Argon
5.1% Oxygen

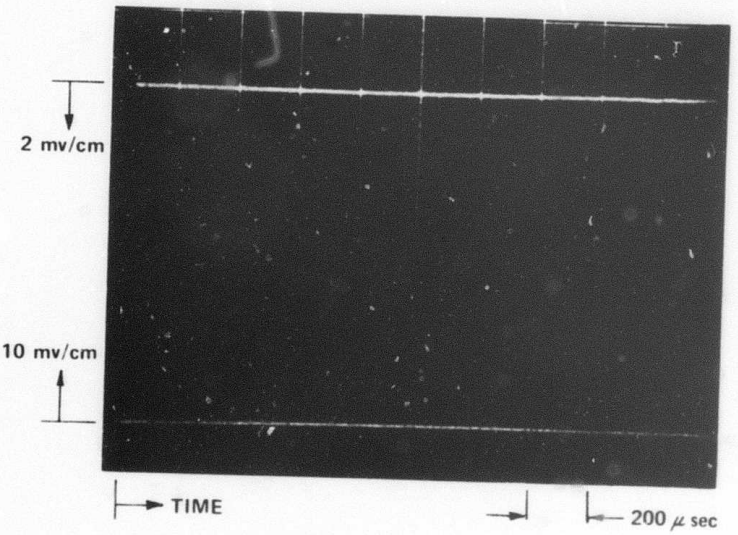

b) WITHOUT A ℓ IN TEST GAS

Figure 2. Incident shock AtO distribution.

The results of Figure 2(a) illustrate that the signals received from each of the observation stations were not of equal magnitude. This is in part due to the geometry of the system. After correcting these data using the calibration data mentioned above, the variation in AlO concentration with distance along the shock tube was on the order of 10 to 15 percent.

2.2 LIQUID-NITROGEN COOLED REFLECTED-SHOCK TEST SECTION

Figure 3 is a schematic of the liquid-nitrogen cooled reflected-shock test section used for the measurements described herein. It has an inside diameter of 2-in. and is approximately 2-in. in length. As shown on Figure 3, liquid nitrogen (under pressure) first flows into a reservoir which contains a light trap, then through the internal passages of the test section, into a hollowed copper block which is in contact with the detector vacuum shroud, and finally exhausts to the atmosphere. Approximately 60 liters of liquid nitrogen are required to cool the system to an acceptably low temperature.

The test section is made of stainless steel, and is held in sandwich-fashion at the end of the shock tube. It is thermally decoupled from the shock tube by thin stainless steel bands. All components are designed to keep the shock-tube walls smooth and continuous. Indium seals and RTV* have been found to be effective vacuum sealants capable of the thermal cycling involved in the experiments.

After the test section had been installed and the vacuum integrity verified, a mold was constructed around the unit and ECCOFOAM EPH insulating foam was poured in order to provide external insulation. The foam density selected for this purpose was approximately 2 lbs/ft^3.

The very low wall temperature over the last two inches of the shock tube could have produced, at worst, a very local effect on the temperature of the driven gas prior to shock heating. As noted above, the cold section of the tube was surrounded by insulation as shown in Fig. 3 and a stainless steel band was used to provide a thermal barrier between the cold section and the

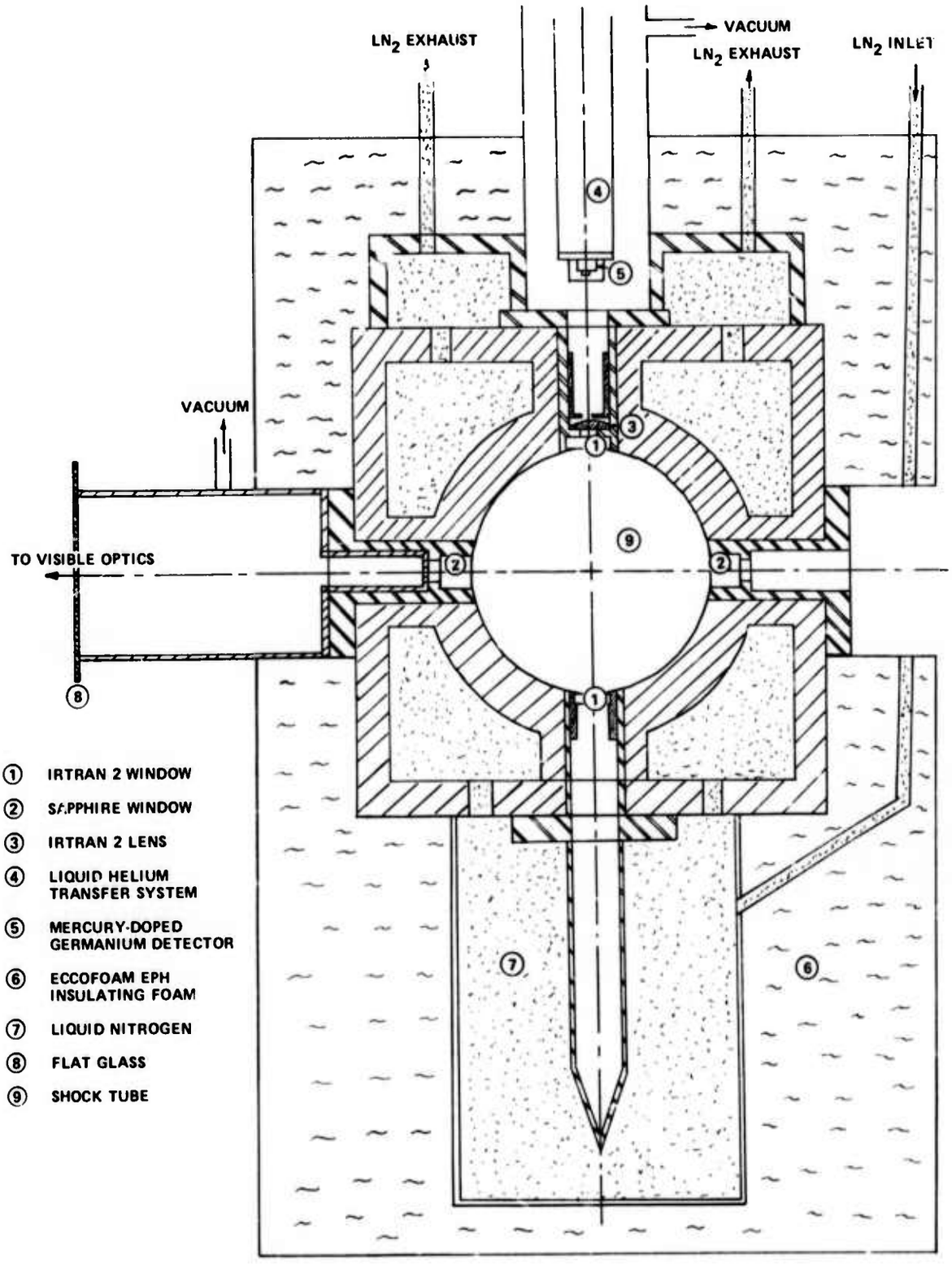

Figure 3. Schematic of LN_2 cooled test section.

remainder of the shock tube. This proved to be an effective barrier because at a location 4 inches upstream of the cold section-shock tube junction the wall temperature was approximately room temperature. That portion of the test gas that comes into contact with the cold wall does so for a time period on the order of one or two minutes. This is not sufficient time for the gas to be significantly cooled. Recall that the total tube length was 11.2 ft. and that the density ratio across the reflected shock, ρ ref/ ρ initial, was approximately equal to 12 (see Table 1). A shock-tube wave diagram constructed for this experiment shows that the gas initially contained in the 2-inch long cold section will be compressed into a thin wafer confined to within 0.17 inches of the end wall. A more severe case, assuming that the gas were significantly cooled over a tube length of 6 inches, would still confine the cooled gas to within 0.5 inches of the end wall. At worst, this would set up a thermal gradient between the test gas at 0.5 inches from the end wall and the remainder of the reflected-shock test-gas (approximately 11 inches in length). However, the infrared optics views the test gas at 1.0 inches from the end wall (see Fig. 1) and it is doubtful that significant heat transfer would occur in the 150 μ sec test period so as to influence the measurements.

The possibility of heating of the Irtran 2 window by energy exchange with the reflected-shock heated gas was also considered. These calculations suggested that the maximum possible (not probable) temperature of the window surface would be 100°K during the test-time. The radiation level associated with this background is at least a factor of 1000 less than the experimental measurements. It was therefore concluded that window surface heating was not a problem for this experiment.

2.3 INFRARED RADIATION DETECTOR SYSTEM

The infrared detector used in these experiments was a liquid-helium cooled mercury-doped germanium detector. The detector was cooled to approximately 4°K prior to performing the experiments. As illustrated in Figure 3, a 1 mm diameter aperture was placed between the detector and Irtran 2 plano-convex lens with a focal length of 1 inch. This arrangement effectively focussed the detector onto the opposite wall of the shock tube and into the

TABLE 1. RESULTS FOR ALO MEASUREMENTS

			0.4854 - 0.4867 μm		0.4871 - 0.4905 μm		10.26 - 11.37 μm		.4856 - .4867	.4871 - .4905
$P_{INITIAL}$	$P_{REF}/P_{INITIAL}$	$T_{REF.}$	$(\mathcal{E}_{VIS})_1$ $\int F_\omega I_\omega d\omega]_{EXPT.}$	$(\mathcal{T}_{VIS})_1$ $\left[\frac{\int F_\omega I_\omega d\omega}{f_{el} P_{ALO}}\right]_{CALC}$	$(\mathcal{E}_{VIS})_2$ $\int F_\omega I_\omega d\omega]_{EXPT.}$	$(\mathcal{T}_{VIS})_2$ $\left[\frac{\int F_\omega I_\omega d\omega}{f_{el} P_{ALO}}\right]_{CALC}$	$\mathcal{E}_{IR}$ $\int F_\omega I_\omega d\omega]_{EXPT.}$	$\mathcal{T}_{IR}$ $\left[\frac{\int f_\omega I_\omega d\omega}{P_{ALO} \kappa_{0,1}}\right]_{CALC}$	$\alpha_{0,1})_{T_0}$	$\alpha_{0,1})_{T_0}$
Torr	—	°K	$\frac{watts}{cm^2\ SR}$	$\frac{watts}{cm^2\ SR\ atm.}$	$\frac{watts}{cm^2\ SR}$	$\frac{watts}{cm^2\ SR\ atm.}$	$\frac{watts}{cm^2\ SR}$	$\frac{watts}{SR}$	$cm^{-2} atm^{-1}$	$cm^{-2} atm^{-1}$
25	11.9	4610	0.063	1465	0.16	3160	6.2×10^{-4}	2.35×10^{-4}	1840	1560
25	11.8	4550	0.026	1310	0.07	3020	3.1×10^{-4}	2.37×10^{-4}	1980	1690
25	11.8	4575	0.048	1330	0.13	3060	5.1×10^{-4}	2.36×10^{-4}	1800	1530
50	10.8	4130	0.028	915	0.07	2000	4.4×10^{-4}	2.48×10^{-4}	1740	1520
50	10.6	4090	0.038	875	0.097	1890	5.6×10^{-4}	2.49×10^{-4}	1550	1320
								AVG:	1780 ± 215	1520 ± 190

AVERAGE VALUE OF $\alpha_{0,1})_{T_0}$ OVER BOTH WAVELENGTHS = 1650 ± 200 $cm^{-2} atm^{-1}$

NOTE:

(a) The values for $\alpha_{0,1})_{T_0}$ quoted above have all been calculated using a value of $f_{el} = 3 \times 10^{-2}$. To find $\alpha_{0,1})_{T_0}$ for other values of f_{el}, multiply given $\alpha_{0,1})_{T_0}$ by $(\text{new } f_{el} / 3 \times 10^{-2})$

(b)

$$\frac{\mathcal{E}_{VIS}}{\mathcal{T}_{VIS}} = f_{el}\ P_{ALO} \quad \text{and} \quad \frac{\mathcal{E}_{IR}}{\mathcal{T}_{IR}} = \alpha_{0,1})_{T_0}\ P_{ALO} \quad \therefore \alpha_{0,1})_{T_0} = f_{el} \cdot \frac{\mathcal{T}_{VIS}}{\mathcal{T}_{IR}} \cdot \frac{\mathcal{E}_{IR}}{\mathcal{E}_{VIS}}$$

cold light trap. It was later found that an Irtran window placed over the trap entrance was more convenient to use and did not compromise the required background signal of the detector. All of the Irtran components were anti-reflecting coated for 8-14 μm. The Irtran 2 windows and lens are all cooled to liquid nitrogen temperatures by the thermal conduction of their mountings. The shroud surrounding the mercury-doped germanium detector and the liquid-helium cold finger is evacuated to 1 x 10^{-6} torr prior to initiation of liquid-nitrogen flow in the test section or liquid-helium flow in the cold finger. The infrared filter is in contact with the cold finger and is thus also cooled to approximately 5°K. Figure 4 presents the transmission characteristics of the infrared filter used for the AlO measurements reported here. The half power points for this particular filter are 10.26 to 11.37 μm. This same filter was used for the uranium/oxygen measurements.

In a previous set of calibaration experiments using the same infrared detector and a liquid nitrogen cooled background, a platinum wire (0.0001 inch in diameter by 0.100 inch in length) of known resistance was placed in thermal contact with the background. The resistance of this wire and the infrared detector signal were monitored as a function of time during the cool-down period. After approximately 2 to 3 hours, during which liquid nitrogen was continually flowing through the system, the wire resistance corresponded to the 77°K value. This value was independently verified by submerging the wire assembly in liquid nitrogen. Continued cooling changed neither the resistance of the wire nor the infrared background-signal (d.c.) level. This signal level was very stable as a function of time, once the wall temperature reached 77°K.

The Irtran 2 window was in thermal equilibrium with the cold sidewall. There was only a very thin (less than 0.002 in) layer of adhesive (RTV 732) between the window and the sidewall which could not support a thermal gradient. The room side of the infrared window was enclosed in a shroud and evacuated to less than 1 x 10^{-6} torr as mentioned above.

The system used in these studies is estimated to be background limited below 100°K. In the AlO studies, the gas radiance itself only corresponded to some 260°K. This high overall system detectivity provides a broad latitude in required optical densities, wavelength bandpass and gas temperature as well as flexibility to the study of other species. This is, in fact, why this unique test section was implemented.

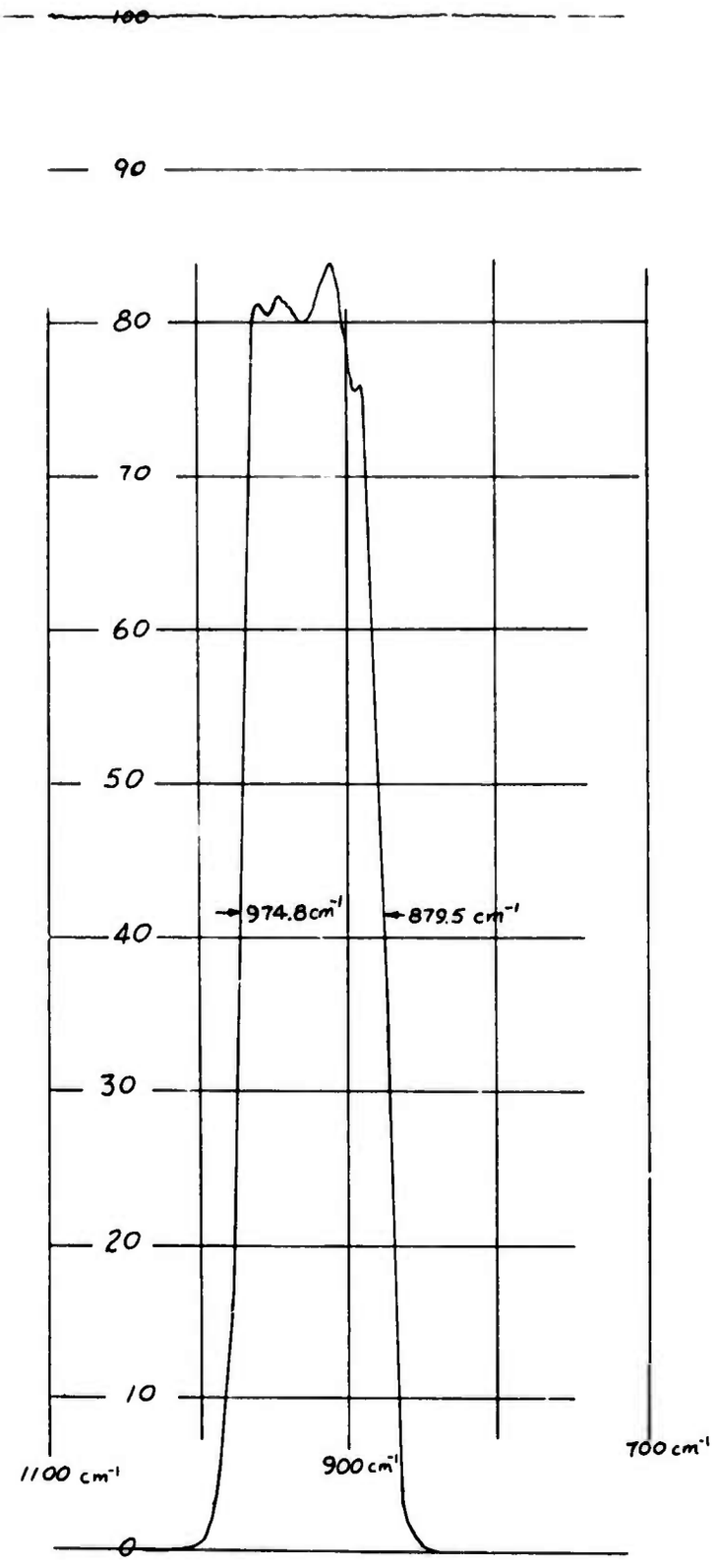

Figure 4. Transmission characteristics of infrared filter. (Supplied by Optical Coating Laboratories, Inc.)

2.4 VISIBLE RADIATION DETECTORS

Figure 5 illustrates the optical apparatus used to monitor the visible radiation intensity in the reflected-shock gas. Sapphire windows were mounted in the shock-tube sidewalls as shown. Because of the cold test section, it was necessary to prevent condensation and subsequent ice formation on the external side of these windows. To accomplish this, an evacuated glass envelope was placed between the cold section and the photomultiplier tube as shown. Two displaced apertures of 1 mm diameter were used to define the beam and determine the amount of light received by the phototubes.

The (0,0) and (1,1) transitions of AlO were monitored in the reflected-shock gas by placing filters with half-power points at approximately 4854 to 4867 A and at 4871 to 4905 A (see Figures 6 and 7 for transmission characteristics) in the field of view of the detectors as shown in Figure 5.

2.5 CALIBRATION OF DETECTOR SYSTEMS

2.5.1 Infrared-Radiation Detector (and 10.26 to 11.37 μm Filter)

In order to calibrate the infrared system, a glass-substrate silvered mirror approximately 7/16-in. by 1/4-in. was mounted at 45° relative to the shock-tube axis on a metal sting so that it could be moved into and out of the field of view of the detector. With the mirror at 45° and in the field of view, the entire upstream shock-tube served as a background cavity at room temperature. When the mirror was retracted, the detector viewed the liquid-nitrogen cooled light trap. The shock tube is considered to provide a blackbody cavity source at the ambient wall temperatures, independent of any properties of the wall, such as emissivity, roughness, etc. The basic principles behind this concept are well-known and embodied in the design of commercial blackbody standards. An appropriate discussion can be found in the "Handbook of Military Infrared Technology", 1965, pages 32-38. It is clearly shown there that a cylindrical cavity with a length/radius ratio of 100, (which the shock tube provides) has an effective emissivity well within a couple percent of unity. This technique is both simple and effective, limited only by the requirement of system response linearity over the range of radiances between the source being measured, and that corresponding to 300°K. Where in question, this linearity can be separately

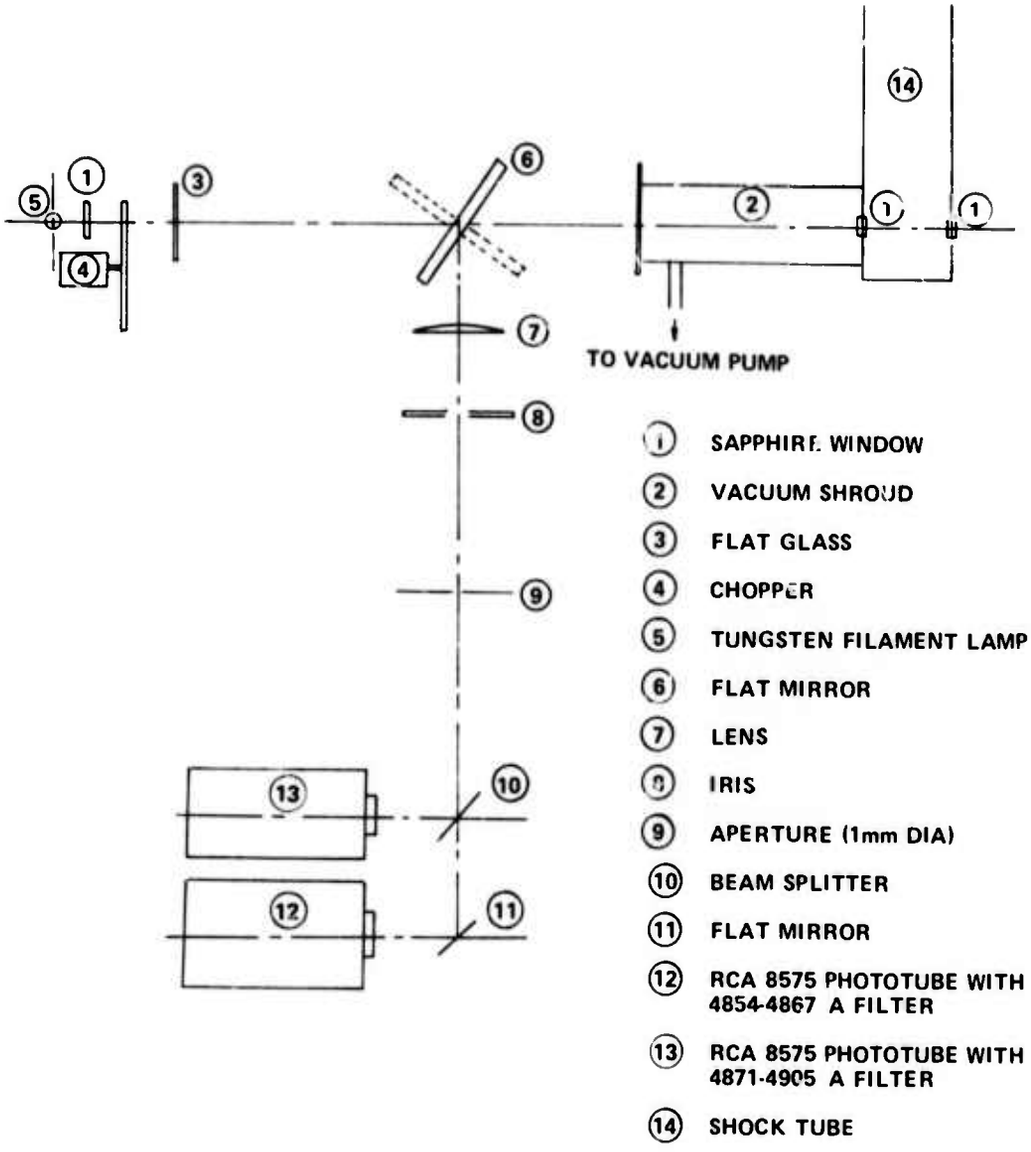

Figure 5. Schematic of reflected-shock optical apparatus.

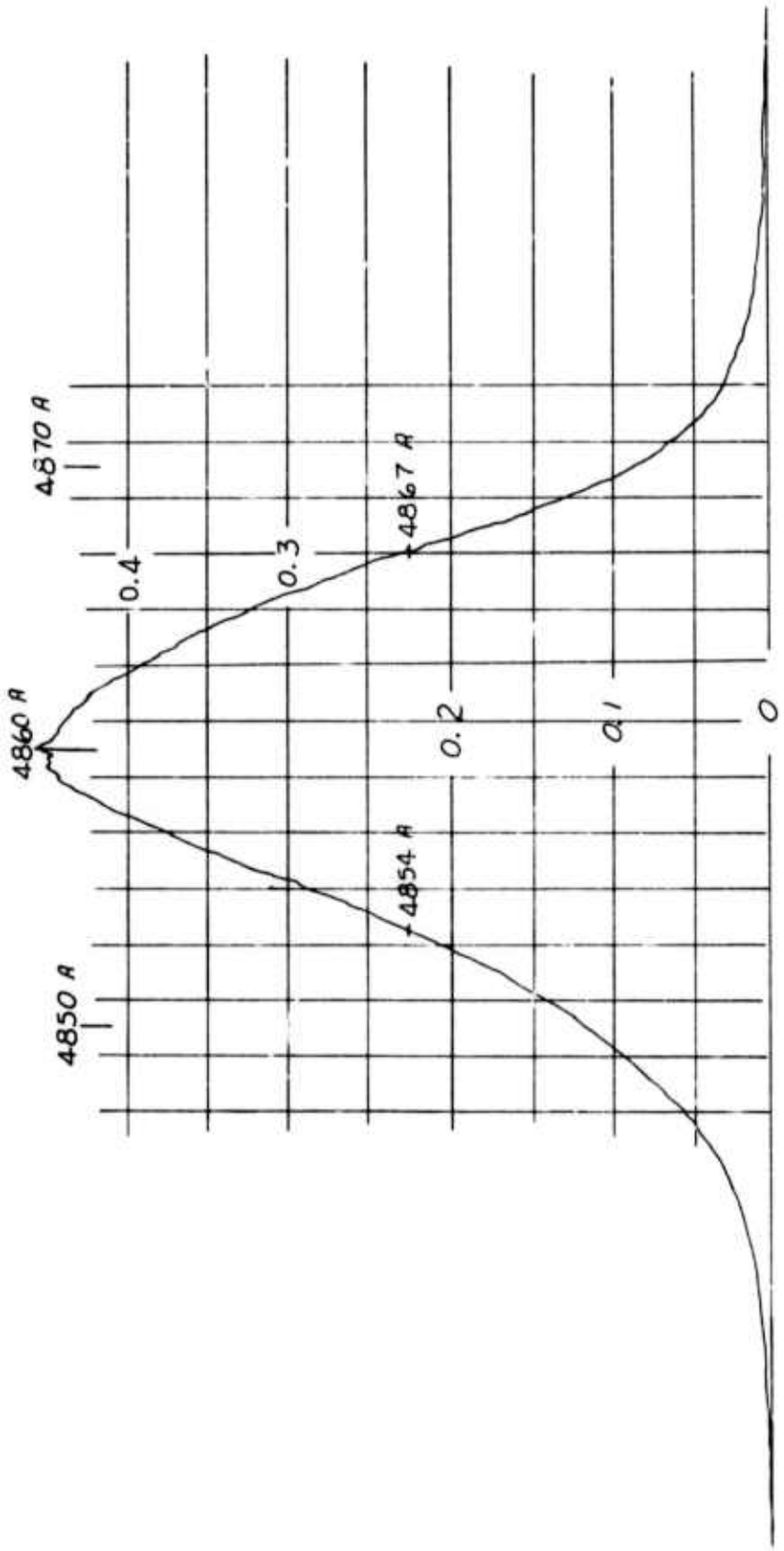

Figure 6. Transmission characteristics for 4854 to 4867 A filter.
(Supplied by Corion Corp.)

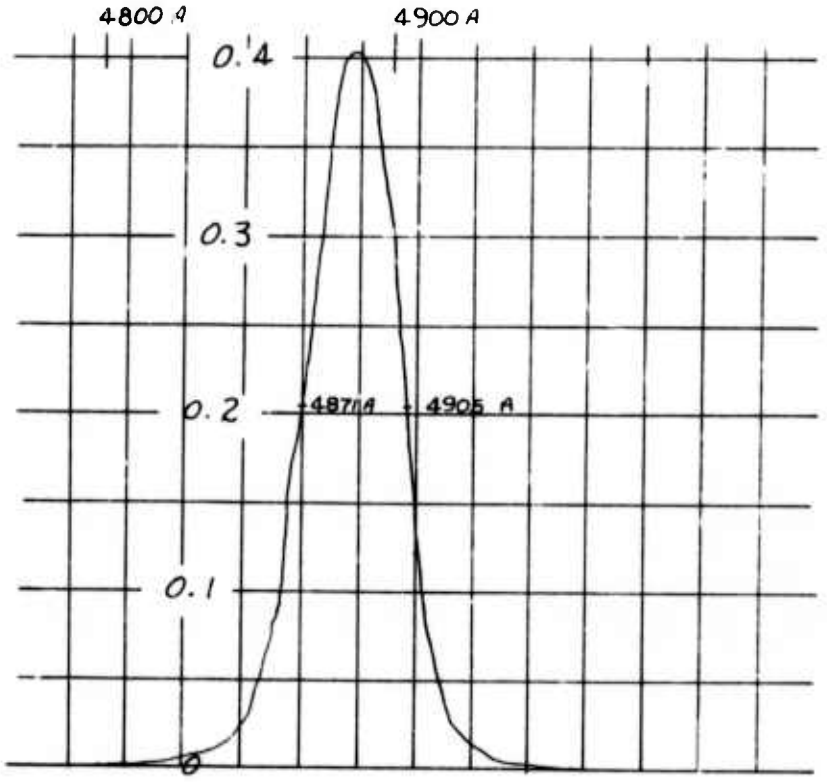

Figure 7. Transmission characteristics for 4871 to 4905 A filter. (Supplied by Corion Corp.)

checked, as was, in fact, done for this system. In this case, however, only a factor of 2 was involved between test gas and calibration radiances.

Because the mirror is not in thermal equilibrium with the walls, its' optical properties must be considered. Being near 80°K, its self-emission is nil; however its reflectivity does moderate the blackbody radiation, and a careful error analysis requires a knowledge of its value. The reflectivity of the mirrors used in the calibration experiments was measured and found to be 87% ±2%. This reflectivity measurement was performed using a Perkin-Elmer, Model 457 infrared spectrophotometer equipped with a Model 134 Barnes horizontal specular reflectance attachment in both sample and standard beams. The standard was a Laser Optics flat mirror coated with Max R coating and its reflectance was 99.4% at 10.6 μm.

Thus the maximum possible error (not probable error) can be estimated as follows:

1. Departure from $\epsilon = 1$ blackbody conditions: -2%
2. Shock tube walls at ±3°F (±1°K): ±1.5% I_{BB}
3. Uncertainity in mirror reflectivity: ±2%

   Then the calibration could be off by $^{+3.5\%}_{-5.5\%}$

Figure 8 is typical of the results obtained with the infrared system using this technique and illustrates that the 293°K background results in a detector output signal of approximately 96 mv. For a mirror reflectivity of 0.87 the spectral radiation intensity corresponding to this signal is approximately 8.31×10^{-4} watts/SR cm^2.

2.5.2 Visible-Radiation Detectors (and 4854-4867 A Filter and 4871-4905 A Filter)

A tungsten ribbon lamp placed external to the shock tube (see Fig. 5) was used as the source of radiation for this calibration. The current flow through the ribbon was changed in discrete steps and the detector output recorded at each steady-state current flow. An optical pyrometer (0.655 μm) was then used to

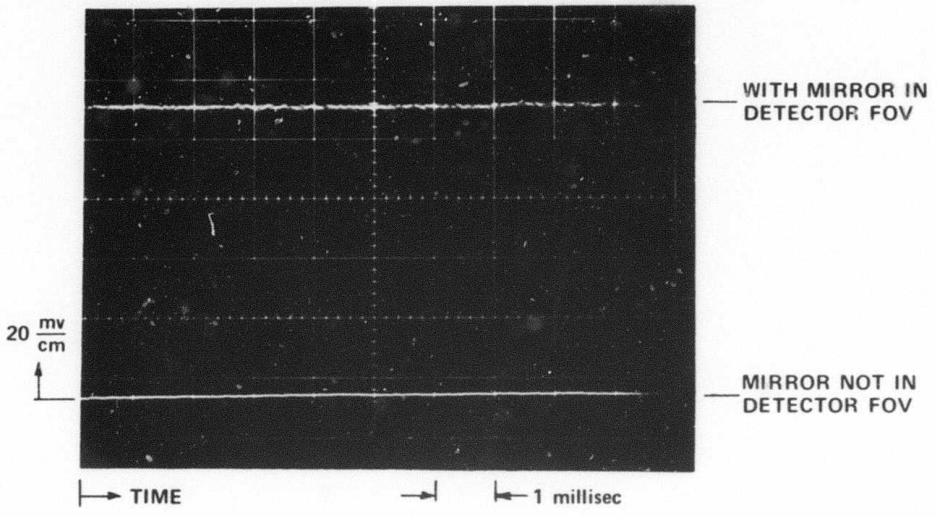

Figure 8. Calibration data for infrared detector and 10.26 to 11.37 μm filter.

determine the ribbon brightness temperature from which the black-body temperature could be determined for each current setting. The brightness temperature at 4860 A and at 4888 A was calculated by making use of the spectral emissivity of tungsten[5,6]. The spectral radiant intensity of the tungsten ribbon was then calculated using the usual Planck functions.

2.6 TEST GAS

The test gas (driven-tube gas) used in all of these experiments was 94.9% Ar plus 5.1% O_2 purchased from Air Products and Chemicals, Inc. A certified chemical analysis of the test gas indicated the following impurity levels:

Acetylene	< 0.05 ppm
Carbon Dioxide	< 0.5 ppm
Carbon Monoxide	< 1.0 ppm
Hydrogen	< 2.0 ppm
Methane	< 0.5 ppm
Nitrogen	< 2.0 ppm
Nitric Oxide	< 0.1 ppm
Total Hydrocarbons	< 0.2 ppm
Water	< 0.15 ppm

SECTION 3

DATA REDUCTION PROCEDURE AND RESULTS

Experimental results have been obtained with the apparatus previously described. These measurements include absolute radiative intensities in the Blue-Green system (B-X transition) of AlO , with data being taken in the wavelength regions 4854-4867 A and 4871-4905 A (these are half-power points of the filters). The 4854-4867 A filter encompasses only portions of the (0,0) and (1,1) bands while the 4871-4905 A filter encompasses tails of the (0-0), (1-1), (2-2), (3-3), (4-4), and (5-5) bands of this system. The relative contributions of the separate bands are determined by analysis, so that from the measurement a determination can be made of the product of AlO concentration and the f-number for the $B \rightarrow X$ transition. Several[7-10] f-numbers for this system have been published; any of these, coupled with the experimental measurement provides a determination of the AlO concentration. Typical results indicate that about 50% of the aluminum that is initially contained in the exploded wire ends up in the test gas. For the conditions of the experiment, the ratio of the Al concentration to that of AlO is approximately 9.

Absolute intensity measurements were also performed in the infrared region (10.26 to 11.37 μm) where the fundamental of the ground state provides a strong radiation source. Again by analysis, this intensity measurement can be used to determine the product of the AlO concentration and the band strength ($\alpha_{o,1}$) of the fundamental. Given the AlO concentration from the $B \rightarrow X$ measurements, a band strength value can be determined. A more detailed description of the data reduction procedure is included in the following paragraphs.

3.1 DATA REDUCTION PROCEDURE

3.1.1 Relation of Radiation Measurements and Transition Probabilities

As noted above, the experimental results in the infrared provide a radiant power per cm^2 of viewing surface per steradian that is observed through a given filter. This measured radiation is equal to

$$R = \int_{\substack{\text{FILTER} \\ \text{RANGE}}} F_\omega I_\omega \, d\omega \quad (\text{watts} / cm^2 \, SR) \tag{1}$$

where

ω = wavenumber (cm^{-1})

F_ω = filter transmission

and

I_ω = spectral radiance from the gas ($\frac{\text{watts}}{cm^2 \text{ ster } cm^{-1}}$).

We wish to derive from this measurement a value for the factor $(\alpha_{0,1})_{T_o} P_{AlO}$, where

$(\alpha_{0,1})_{T_o}$ = integrated absorption coefficient of the (0,1) band of the fundamental sequence at standard temperature (T_o) per atmosphere of AlO (cm^{-2} atm^{-1})

and

P_{AlO} = partial pressure of AlO (atm).

If the gas can be treated as optically thin, this can be accomplished through the relation

$$I_\omega = \sum_{\text{BANDS}} (P_{\omega_{v'',v''+1}})_{T_G} \, l \, (I_{EB_\omega})_{T_G} \tag{2}$$

where

$(P_{\omega_{v'',v''+1}})_{T_G}$ = spectral absorption coefficient at wave number ω for a given band (cm^{-1})

T_G = gas temperature

ℓ = path length (cm)

$(I_{BB_\omega})_{T_G}$ = spectral blackbody intensity ($\frac{\text{watts}}{cm^2\ \text{ster}\ cm^{-1}}$)

The quantity $(P_{\omega_{v'',v''+1}})_{T_G}$ can be calculated in terms of $(\alpha_{v'',v''+1})_{T_G}$ for each band that contributes within the range of the filter, viz. (1,0) through (11,10), using the relation by Penner, Sepucha and Lowder[11],

$$(P_{\omega_{v'',v''+1}})_{T_G} = [\alpha_{v'',v''+1}]_{T_G}\, P_{REF}\, \frac{hc}{4kT_G B_{v''}}\, \frac{|\Delta\omega|\left[1 \pm \frac{|\Delta\omega|}{\omega}\right]}{\left[1 \mp |\Delta\omega|\frac{\alpha_e}{2B_{v''}^2}\right]\left[1 \mp (|\Delta\omega| \pm 2B_{v''})\frac{\alpha_e}{4B_{v''}^2}\right]}$$

$$\times \exp\left[-\frac{hc}{4kT_G}\, \frac{|\Delta\omega|\left\{|\Delta\omega| \mp 2B_{v''}\left[1 \mp (|\Delta\omega| \pm 2B_{v''})\frac{\alpha_e}{4B_{v''}^2}\right]\right\}}{B_{v''}\left[1 \mp (|\Delta\omega| \pm 2B_{v''})\frac{\alpha_e}{4B_{v''}^2}\right]^2}\right]$$

$$\times \left\{\frac{1 - \exp\left[-(hc/kT_G)(\omega \pm |\Delta\omega|)\right]}{1 - \exp\left[-hc\omega/kT_G\right]}\right\} \qquad (cm^{-1}\,atm^{-1}) \tag{3}$$

where

$|\Delta\omega|$ = wavenumber displacement from band origin (cm^{-1})
(Where a band head occurs, the displacement for $|\Delta\omega| > |\Delta\omega|_{HEAD}$ is the sum of the displacements to the band head and from the band head.)

and $B_v = B_e - \alpha_e\left(V + \frac{1}{2}\right)$

where B_e and α_e are rotational constants (cm^{-1}).

The upper sign in Equation (3) corresponds to the R branch and the lower sign to the P branch.

The value of $(\alpha_{v'',v''+1})_{T_G}$ can be related to $(\alpha_{0,1})_{T_o}$ by the relation (see Penner[12], p. 141)

$$(\alpha_{v'',v''+1})_{T_G} \cong (\alpha_{0,1})_{T_0} \frac{(\bar{\omega}_{v'',v''+1})_{T_G}}{(\bar{\omega}_{0,1})_{T_0}} \frac{|R_{v'',v''+1}|^2}{|R_{0,1}|^2} e^{-\frac{E_{v''}}{kT_G}+\frac{E_0}{kT_0}} \left(\frac{T_0}{T_G}\right)$$

(4)
$$\times \frac{\left(1-e^{-\frac{hc\,\omega^{\circ}_{v'',v''+1}}{kT_G}}\right)\left(1-e^{-\frac{hc\,\omega^{\circ}_{0,1}}{kT_G}}\right)}{\left(1-e^{-\frac{hc\,\omega_{0,1}}{kT_0}}\right)^2}$$

where

E_v = energy of v^{th} vibrational level (ergs)

$\bar{\omega}_{v'',v'}$ = 'effective' band wavenumber (cm^{-1})

$$\cong \omega^{\circ}_{v'',v'} + (B_{v'} - B_{v''})\left(1 + \frac{kT_G}{hcB_{v''}}\right)$$

$$+ (B_{v'} - B_{v''}) \frac{[1+\exp(-hc\,\omega^{\circ}_{v'',v'}/kT_G)]}{[1-\exp(-hc\,\omega^{\circ}_{v'',v'}/kT_G)]}$$

$\omega^{\circ}_{v'',v'}$ = wave number at band origin (cm^{-1})

and the ratio of the squares of the vibrational matrix elements (Heaps and Herzberg[13]) is

(5)
$$\frac{|R_{v'',v'+1}|^2}{|R_{0,1}|^2} = (V''+1) \frac{\left(\frac{1}{\chi_e}-2\right)^2 \left(\frac{1}{\chi_e}-2V''-3\right)\left(\frac{1}{\chi_e}-2V''-1\right)}{\left[\frac{1}{\chi_e}-2(V''+1)\right]^2 \left(\frac{1}{\chi_e}-V''-1\right)\left(\frac{1}{\chi_e}-3\right)}$$

where χ_e = ratio of vibrational constants, $\frac{\omega_e \chi_e}{\omega_e}$

Finally, then, the measured radiation, R , can be related to $(\alpha_{0,1})_{T_0} P_{RLO}$ by combining Equations (1) and (2):

$$R = \int_{\substack{\text{FILTER}\\ \text{RANGE}}} F_\omega \sum_{\text{BANDS}} [(P_\omega)_{T_G}]_{\text{BAND}}\, \ell\, (I_{BB_\omega})_{T_G}\, d\omega$$

(6)
$$= \left\{(\alpha_{0,1})_{T_0} P_{RLO}\right\} \left\{\ell \int_{\substack{\text{FILTER}\\ \text{RANGE}}} F_\omega\, (I_{BB_\omega})_{T_G} \sum_{\text{BANDS}} \frac{[(P_\omega)_{T_G}]_{\text{BAND}}}{(\alpha_{0,1})_{T_0} P_{RLO}}\, d\omega\right\}$$

and calculating the quantity in the second bracket using Equations (3) through (5).

The quantity $\left(P_{\omega_{v'',v''+1}}\right)_{T_G}$ was calculated at 10 cm^{-1} intervals of ω for bands (1,0) through (11, 10) and summed over the bands. The integral was then performed over the filter range, including contributions to the point where the transmission fell to 1/270 of the peak value.

The thin gas approximation can be evaluated by considering the approximate line widths for the rotational lines and the measured intensity of the infrared radiation. The average spacing of the spectral lines which contribute appreciably is about 15 lines per cm^{-1}, and the semi-half-width of the lines is taken as

$$\gamma = 0.06 \frac{\rho}{\rho_o} \sqrt{\frac{T}{T_o}} \quad cm^{-1} \tag{7}$$

The coefficient 0 06 cm^{-1} is an estimate based on data for other molecules[13]. For the test conditions the semi-half-widths are $\sim .09$ cm^{-1} for the 25 torr initial pressures, and $\sim .16$ for the 50 torr initial pressure. Thus the lines are very overlapped, and the gas can be considered grey. The magnitude of the radiation is approximately 0.3% of blackbody in this region. Thus the thin-gas approximation is adequate.

An expression similar to equation (6) can be obtained for the radiation from the Blue-Green system in terms of the electronic f-value. If either the gas is optically thin, or the lines are well separated compared with their line width, the lines can be treated separately so that

$$R = \sum R_\lambda \tag{8}$$

and R_λ is the contribution from the λ^{th} spectral line. Since the lines are much thinner than the filter half-widths, F_ω can be taken as a constant F_λ for any given line, and

$$R_\lambda = F_\lambda \int I_{\omega_\lambda} \, d\omega \tag{9}$$

In the thin gas approximation, the radiation from a single line is given by

$$\int I_{\omega_i} \, d\omega = f_{el} \, P_{AlO} \, C_{el} \left(q_{v'v''} \, \omega_{v'v''}^{4} \, B_{v'} \, e^{-\frac{E_{v'}}{kT}} \right) \left\{ \begin{array}{l} \frac{(K'+1)-\frac{1}{4}}{(K'+1)} \text{ for } P \text{ branches} \\ \frac{(K')^2-\frac{1}{4}}{K'} \text{ for } R \text{ branches} \end{array} \right\} e^{-\frac{EK'}{kT}} \left(\frac{\text{watts}}{\text{cm}^2 \text{SR}} \right) \tag{10}$$

where

$$C_{el} = \frac{10^{-7}}{4\pi} \, l \, \frac{8\pi^2 \epsilon^2}{\mu C} \, \frac{1}{\bar{\omega}} \, (1.01325 \times 10^6) \left(\frac{hc}{kT} \right)^2 \frac{q_{el'} \, e^{-E_{el'}/kT}}{Q_{el} \, Q_v}$$

ϵ = electron charge (e.s.u.)

μ = electron mass (gm)

$q_{el'}$ = degeneracy of upper electronic state

$E_{el'}$ = energy of upper electronic state (ergs)

Q_{el} = electronic partition function

Q_v = vibrational partition function for upper electronic state

$q_{v'v''}$ = Franck-Condon factor

$\omega_{v'v''}$ = wave number of $v'v''$ band head (cm^{-1})

$\bar{\omega}$ = $\sum_{v'} \omega_{v'v''} \, q_{v'v''}$ (cm^{-1})

$E_{v'}$ = energy of upper vibrational level (ergs)

$E_{K'}$ = energy of upper rotational level (ergs)

The measured radiation, R, can then be related to $f_{el} \, P_{AlO}$ by combining equations 8 and 9

$$R = f_{el} \, P_{AlO} \sum_{\substack{\text{all} \\ \text{lines}}} F_i \left(\frac{\int I_{\omega_i} \, d\omega}{f_{el} \, P_{AlO}} \right) \tag{11}$$

where the terms inside the summation are calculated from equation (10) and the known filter transmission at each line i.

To test the accuracy of the thin-gas approximation for the Blue-Green system, the radiance at the center of the strongest line ($K'' = 45$) was calculated, using equation 10 and assuming that the line shape is controlled by pressure broadening. Then

$$I_{o_i} = \frac{1}{\pi \gamma} \int I_{\omega_i} \, d\omega$$

and the semi-half width is again taken as in equation 7. For the low density case (higher temperature) the thin-gas radiance at the center of the line is 35% of blackbody, and the Landenburg Reiche correction factor for the thin gas radiation[14] is $\frac{f(x)}{x} = 0.95$. For the high density (lower temperature) case, where the blackbody radiance is lower, the calculated thin-gas radiance at the center of the line is 62% of blackbody. The Landenburg Reiche factor is $\frac{f(x)}{x} = 0.85$. Thus for the visible radiation some small correction to the thin-gas results should be made. However, the examples chosen above were for the strongest line, and the magnitude of the correction indicated does not warrant a more detailed analysis at this point. The radiation in the band-head region, where the line strengths are weaker (but the lines are overlapping) has a lower average emissivity (about 0.07 for the high temperature and about 0.2 for the low temperature) than at the centers of the strong lines, and would not require a correction to the thin-gas formulas. In so far as such corrections would reflect in the final result, they would decrease the quoted value of the infrared transition probability. It appears that the correction would be much too small to reconcile the consistent 15% difference in the values of α obtained with the two different visible filters (see Table 1).

3.1.2 Determination of Reflected-Shock Temperature and Thermochemical Calculations

The reflected-shock temperature was determined in the following manner. First, the shock-wave transit time was measured over four intervals and extrapolated to the end wall as shown on Figures 9 and 10 which are x-t diagrams for both the 25-torr and 50-torr experiments. The electronic counters used in these measurements are accurate to within ± 1 μsec. Typical transit times were on the order of 360 to 380 μ sec and thus the possible error in transit times results in an error in shock velocity of less than 0.3%. The validity of extrapolating the shock-wave transit time to the end wall was independently tested by locating an ionization gauge in the end wall and recording the transit time over the last interval. The conclusion of these experiments was that the linear extrapolation to the end wall is an excellent approximation for this shock tube and these experimental conditions. The aluminum in the initial test gas was assumed to be Al_2O_3 (S) of a known

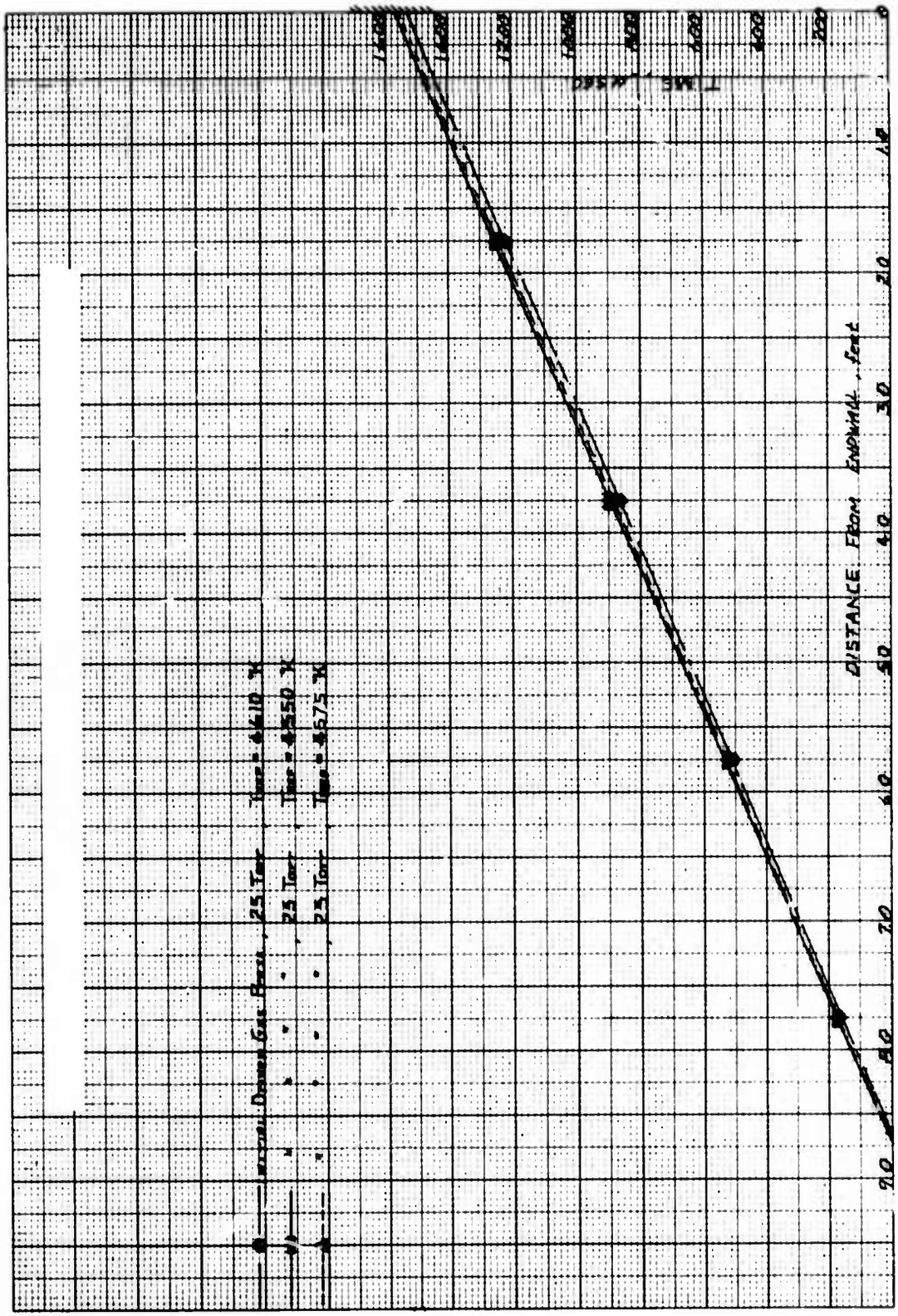

Figure 9. X-7 diagram for 25-torr AtO experiments.

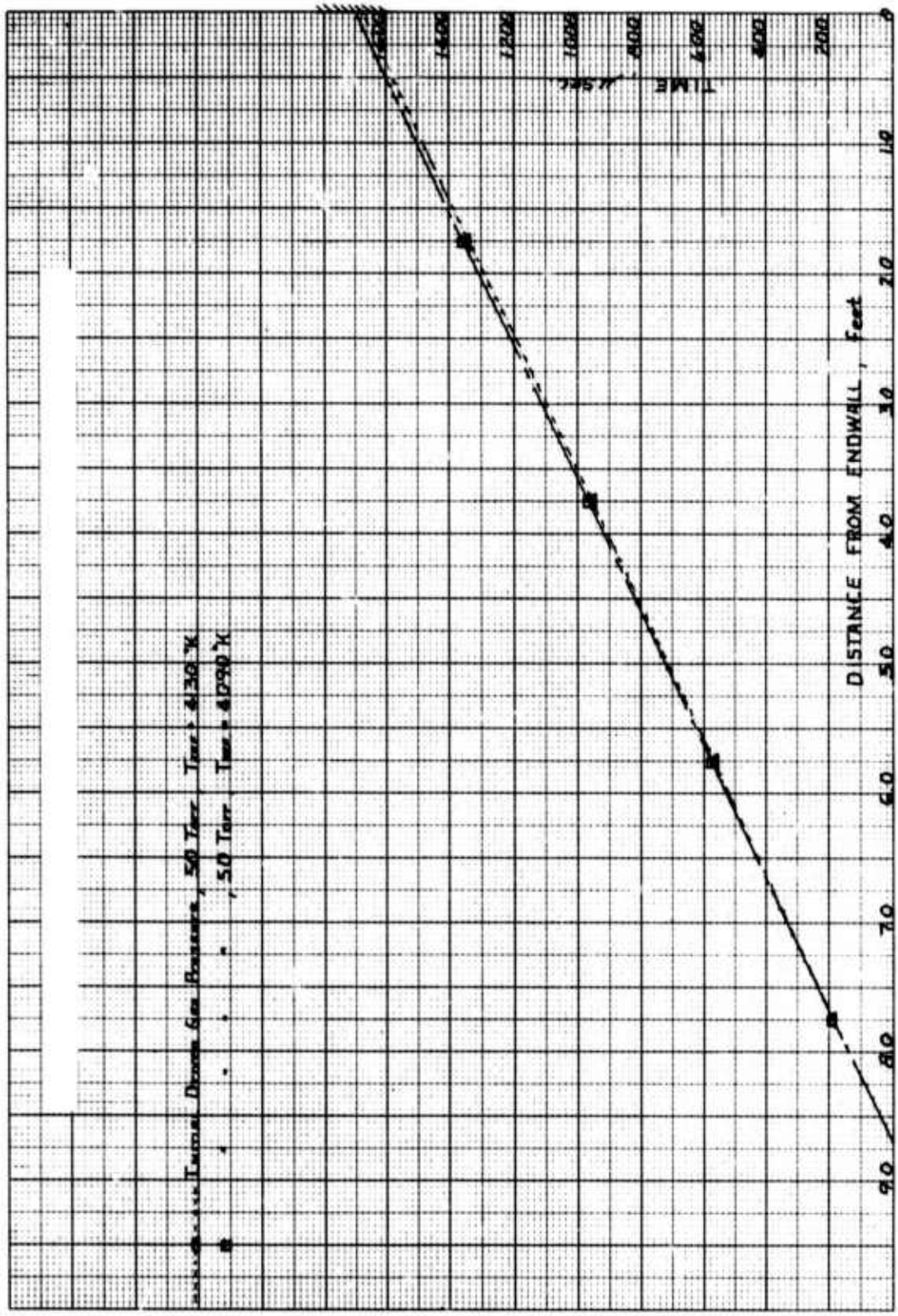

Figure 10. X–τ diagram for 50-torr $A(^1)$ experiments.

maximum amount. The machine program used to calculate the reflected-shock temperature as a function of shock-wave velocity and initial pressure included the thermochemistry of the reaction Al_2O_3 (S) $\rightarrow$ Al_2O_3 (g) and the necessary subsequent gas-phase reactions. The calculation must be performed for various amounts of the wire (Al_2O_3) getting into the initial test gas. Recall that the data reduction procedure provides an estimate of the AlO partial pressure through the value $f_{\ell\ell}\ P_{alo}$ (Broida's value for $f_{\ell\ell}$ was used). It is thus necessary to iterate on the partial pressure and the reflected-shock temperature in order to arrive at the correct reflected-shock temperature. The reflected-shock temperatures determined in the manner outlined above are accurate to within 1%.

The thermochemical data used in the data reduction procedure was the JANAF table revisions dated 1971. The equilibrium reflected-shock calculations indicate that the AlO concentration is changing rapidly (approximately a factor of 10) in the temperature range 4150 to 4750°K. However, it must be pointed out that the experimental results reported here do not rely on the absolute value of the AlO concentration in the data reduction procedure. The parameter that is important is the ratio of the AlO blue-green band radiation to the AlO infrared radiation, ($\mathcal{T}_{VIS}$ / $\mathcal{T}_{IR}$) which is plotted in Figure 11. It is demonstrated that over the temperature 4090 to 4610°K the ratio of blue-green to infrared changes by a factor of approximately 1.8 which is far less than the previously mentioned variation in the AlO concentration.

3.2 DISCUSSION OF AlO RESULTS

Before initiating the aluminum oxide measurements, several experiments were performed to be certain that the radiation observed in the visible and infrared spectral regions was due to the combined presence of oxygen and aluminum. Measurements were obtained with the driven-tube gas composed of (a) pure argon (b) argon plus aluminum and (c) 94.9% argon plus 5.1% oxygen. Coupled with the known spectral purity of the system, the results of these experiments demonstrated that the gas radiance was attributable to aluminum oxide.

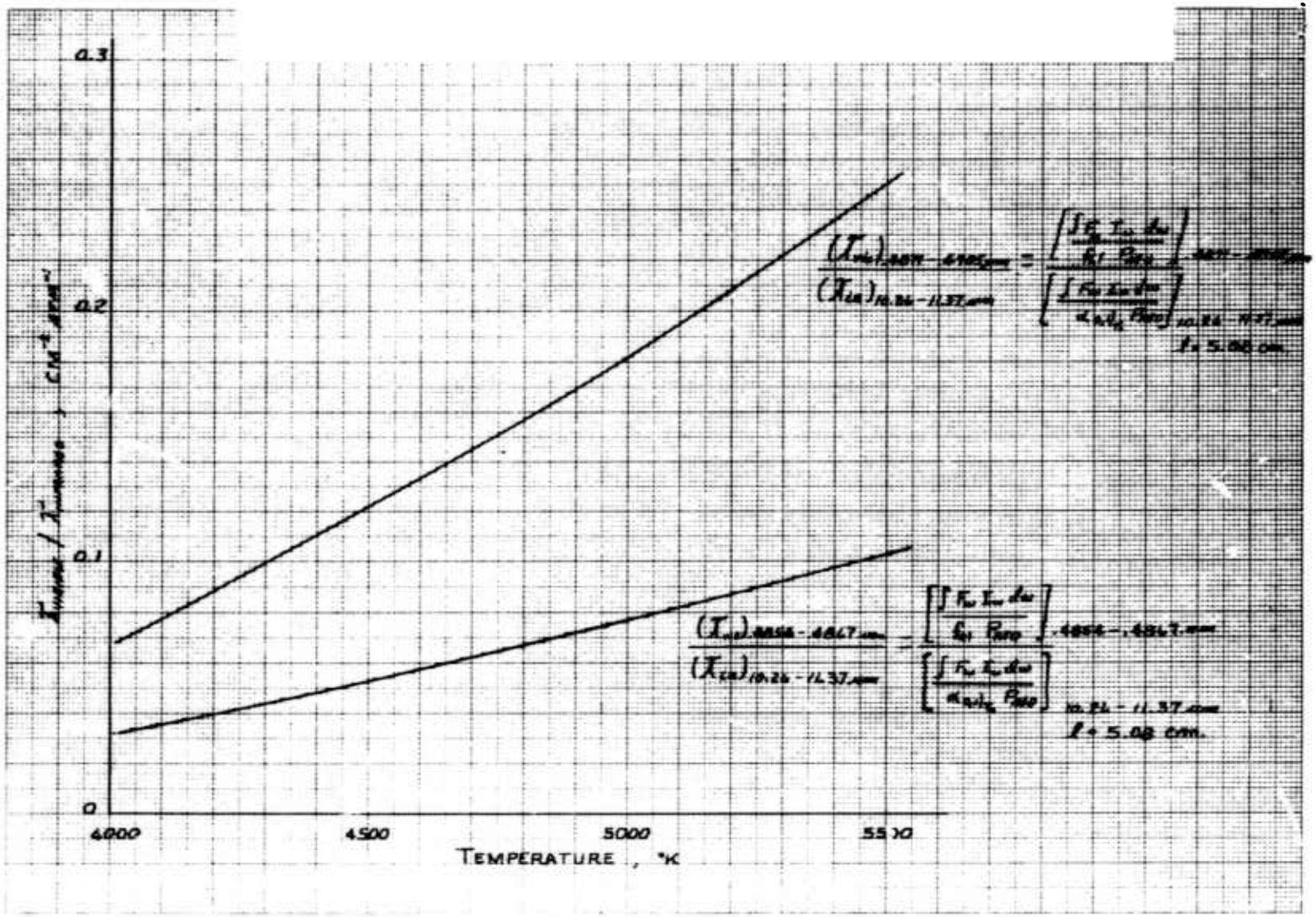

Figure 11. Calculated ratio of AlO blue-green to AlO infrared, τ_{vis}/τ_{IR}.

The band strength ($(\alpha_{o,1})_{T_o}$) of the AlO fundamental in the infrared (10.26 to 11.37 μm) was measured over a reflected-shock temperature range of 4610°K to 4090°K. Typical oscilloscope records obtained simultaneously during the course of the aluminum-oxide measurements are shown in Figure 12. For this particular experiment the test gas was 94.9% argon plus 5.1% oxygen plus exploded aluminum wire at an initial driven-tube pressure of 25 torr. The resulting reflected-shock temperature was 4575°K. Equilibrium reflected-shock calculations performed for the temperature range of 4000 to 5000°K indicate that the aluminum atom concentration was greater than the aluminum-containing molecular species. However, of the molecular species, AlO was dominant followed by Al_2O which is present to approximately 1/1000 of AlO. Figures 12 (a) and 12 (b) are the Blue-Green measurements obtained in the wavelength regions 4854-4867 A and 4871-4905 A. Figure 12(c) is the infrared measurement obtained for the wavelength region 10.26 to 11.37 μm. The detector output signals taken from these records in order to arrive at a value for $(\alpha_{o,1})_{T_o}$ for this experiment were read at the vertical centerline (hatched line) of the photograph.

Table 1 is a summary of the results obtained from the aluminum oxide experiments at two different driven-tube pressures for a temperature range of approximately 4090°K to 4610°K. The values given in this table for $(\alpha_{o,1})_{T_o}$ were obtained using a value of $f_{el} = 3 \times 10^{-2}$ which is felt to be the best currently available value[7]. To find $(\alpha_{o,1})_{T_o}$ for other values of f_{el} it is only necessary to multiply Table 1 values of $(\alpha_{o,1})_{T_o}$ by the ratio $[(\text{new } f_{el})/3 \times 10^{-2}]$.

The arithematic average of the $(\alpha_{o,1})_{T_o}$ values obtained in the wavelength region 4854-4867 A is 1780 $\pm$215 cm^{-2} atm^{-1} whereas the arithmetic average in the 4871-4905 A wavelength interval is 1520 $\pm$190 cm^{-2} atm^{-1}. The average value of $(\alpha_{o,1})_{T_o}$ over the two wavelength intervals provides the value that is felt to be most representative of these experimental results for the $1 \rightarrow 0$ transition, i.e.

$$(\alpha_{o,1})_{T_o} = 1650 \pm 200 \text{ cm}^{-2} \text{ atm}^{-1}$$

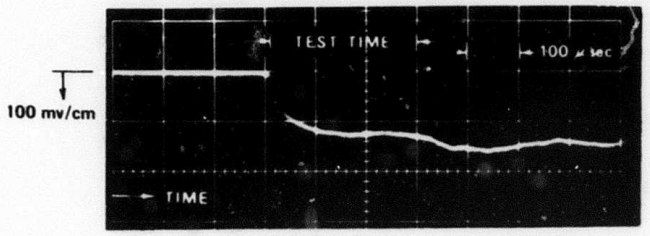

TEST GAS: 25 torr
94.9% Argon
5.1% Oxygen
EXPLODED ALUMINUM WIRE
REFL. SH. TEMP: 4740°K

(a) 4854 TO 4867 A WAVELENGTH REGION

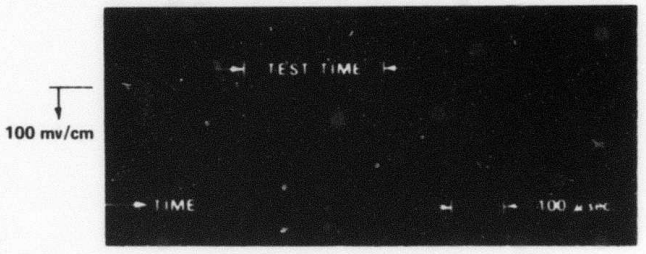

(b) 4871 TO 4905 A WAVELENGTH REGION

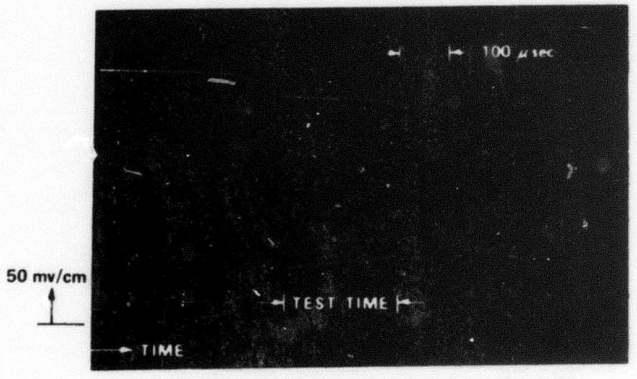

(c) 10.26 TO 11.37 μm WAVELENGTH REGION

Figure 12. Typical oscilloscope records for AlO measurements.

This result can be compared with that recently obtained by Sultzmann[15]

$$(\alpha_{o,1})_{T_o} = 724 \pm 145 \text{ cm}^{-2} \text{ atm}^{-1}$$

The present value of $(\alpha_{o,1})_{T_o}$ is approximately two times larger than that of Sultzmann, and both results are significantly higher than would be inferred from atmospheric release experiments[16]. At the present time, the source of the discrepancy in the experimental numbers is not understood.

3.3 DISCUSSION OF UO_x RESULTS

Earlier reported studies[3,4] have demonstrated that the exploding-wire aerosol shock-tube technique is applicable to the study of radiance from heated $U/O_2/Ar$ mixtures. The uranium vaporization time was measured and shown to be less than 50 μsec, well within the equilibrium test time in the shock tube. It was further demonstrated that the LWIR radiation is likely due to a uranium oxide.

Difficulties encountered in obtaining the previously discussed aluminum oxide band strength in the infrared precluded completion of the proposed plan to measure absolute band strengths in the infrared for uranium/oxygen/argon mixtures. However, it was possible to obtain measurements in the 10.26 to 11.37 μm wavelength region for reflected-shock temperatures comparable with those used in the AlO experiments and in this manner infer the relative importance of UO_x and AlO radiation in the infrared. Figure 13 is typical of the measurements obtained for an uranium/oxygen/argon mixture at an initial driven-tube pressure of 25 torr and a reflected-shock temperature of 4900°K at approximately 6.4 atm pressure. At this reflected-shock condition, the equilibrium species concentrations (in moles/cm^3) of UO, UO_2, and UO_3 were calculated[4] to be approximately equal.

A comparison of this result with Figure 12(c) suggests that the AlO and UO_x radiation intensities are roughly comparable in the 10.26 to 11.37 μm wavelength region. However, two factors must be considered before concluding that the radiation intensities are comparable (1) the relative number of uranium and aluminum particles available for oxidation and (2) the difference in the spectral structure of AlO and the relevant UO_x band heads in the infrared.

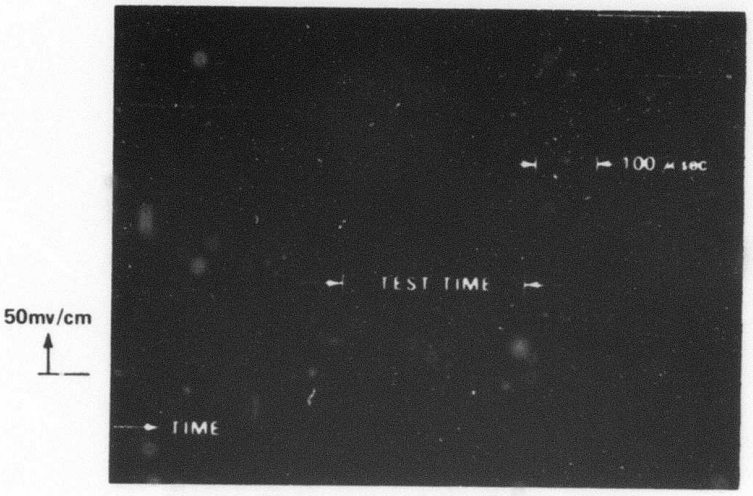

Figure 13. Typical oscilloscope record for UO_x measurements.

Concerning item (1), the aluminum wire used in these experiments was 0.005 inch diameter by 1.0 inches long and the uranium strip was 0.006 inch thick by 0.040 inches wide by 0.75 inches in length. With these dimensions one can calculate that the number of available aluminum atoms is approximately 1.9×10^{19} and the number of available uranium atoms is approximately 1.4×10^{20}. Thus there are approximately seven times more uranium atoms available (to form UO, UO_2 or UO_3) than there are aluminum atoms available (to form AlO). The yield of atoms in the shock tube loading procedure was considered constant.

Concerning item (2), it is important to note that the AlO fundamental is at 10 μm (1000 cm^{-1}), which is relatively close to the shorter wavelength half-power point of the filter (10.26 to 11.37 μm), whereas the UO and UO_2 fundamentals are at 12.2 and 12.9 μm, respectively. The transmissien of the infrared filter used in these experiments is on the order of 1 to 2 percent (see Fig. 4) at the wavelength of the UO fundamental and thus would pass only a small portion of the fundamental radiation. The net contribution of these bands thus depends on the extent to which they are broadened at elevated temperatures. It is thus possible that the UO and UO_2 radiation in the 12.2 to 12.9 μm region would exceed the levels measured for AlO in the 10.26 to 11.37 μm region.

The diagnostic equipment necessary to perform the band-strength measurements for UO_x is available at Calspan. The technique relies on the determination of the U atom concentration form photographed absorption spectra of atomic lines in the visible, using optically thin lines whose f-numbers are known.

A short set of tests to demonstrate the feasibility of this approach to the U system was conducted previously at Calspan[4]. Although the components of the system were not optimized for the feasibility tests, the results indicated that this technique would be of direct applicability to U line studies. The optical system uses a synchronized flash lamp as a bright source of visible continuum irradiance, which passes through an optical train consisting of the shock tube, a shutter and the spectrometer. In Ref. 4 is described a possible method from which absolute band strength measurements can be obtained with the aerosol shock-tube facility. The object is to obtain an exposure on the plate which results primarily from the flash; the radiance from the gas is suppressed below plate response threshold by high flash intensity and a synchronized shutter.

SECTION 4

CONCLUSIONS

The band strength of the AlO fundamental, $(\alpha_{o,1})_{T_e}$, in the infrared (10.26 to 11.37 μm) was found to be 1650 $\pm$200 cm^{-2} atm^{-1} over a temperature range of 4610°K to4090 °K. Experimental difficulties encountered during the course of the program precluded similar quantitative results for the uranium/oxygen system. Qualitatively, the results indicate potentially significant radiance levels when compared to those from AlO .

REFERENCES

1. Nicholls, R.W., Parkinson, W.H., and Reeves, E.M., "The Spectroscopy of Shock-Excited Powdered Solids", Appl. Optics, Vol. 2, 919, (1963).

2. Watson, R., Morsell, A.L., and Hooker, W.J., "Techniques for Conducting Shock Tube Experiments with Mixtures of Ultrafine Solid Particles and Gases", Rev. Sci. Instr., Vol. 38, 1052, (1967).

3. Wurster, W.H., "Semi-Annual Technical Report: "Uranium-Oxygen Radiation Studies", CAL Report No. WB-5117-A-1, 1972.

4. Wurster, W. H., "Uranium-Oxygen Radiation Studies, Final Report", Calspan Report No. WB-5117-A-3, 16 Aug 1974, DNA Report 3398F.

5. Handbook of Chemistry and Physics, 54th Edition, pp. E-216. CRC Press, 1973-1974.

6. deVos, J.C., Physica Vol. 20, 690 (1954).

7. Johnson, S.E., Capelle, G. and Broida, H.P., "Laser Excited Fluorescence and Radiative Lifetimes of AlO J. Chem. Physics, Vol. 56, No. 1, p 663, 1972.

8. Michels, H.H., "Ab Initio Calculation of the $B\,^2\Sigma^+ - X\,^2\Sigma^+$ Oscillator Strengths in AlO", J. Chem. Physics, Vol. 56, No. 1, pp. 665, 1972.

9. Vanpee, M., Kineyko, W.R., and Caruso, R., "Experimental Determination of the Oscillator Strengths for the $A\,^2\Sigma - X\,^2\Sigma$ Band System of

Aluminum Oxide", Combustion and Flame, Vol. 14, p. 381, 1970.

10. Hooker, W.J. and Main, R.P., "AlO (A-X) Oscillator Strengths and Collisional Reaction Rates", Final Report, KMS Technology Center, March 1971.

11. Penner, S.S., Sepucha, R.C. and Lowder, J.E., "Approximate Calculations of Spectral Absorption Coefficients in Infrared Vibration-Rotation Spectra", J. Quant. Spectrosc. and Radiant Transfer, Vol. 10, pp. 1001, 1970.

12. Penner, S.S., Quantitative Molecular Spectroscopy and Gas Emissivities, Addison Wesley Publishing Co., Reading, Mass. 1959.

13. Heaps, H.S. and Hertzberg, G., "Intensity Distribution in the Rotation-Vibration Spectrum of the OH Molecule", Zeitschrift fur Physik, Bd 133, S 48-64, 1952.

14. Ludwig, C.B., Malkmus, W., Reardon, J.E. and Thomson, J.A.L., "Handbook of Infrared Radiation from Combustion Gases," NASA SP-3080, National Aeronautics and Space Administration, Washington, D. C., 1973 Table 5-19.

15. Sulzmann, Klaus G.P., "Shock-Tube Measurements of the f-number for the Fundamental Vibration-Rotation Bands of AlO in the $X^2\Sigma^+$ Electronic Ground State", J. Quant. Specty. and Radiant Transfer, Vol.15, 1975.

16. Private Communication, Forrest Gilmore, R and D Associates, Santa Monica, California 90403.